Heterogeneous Photochemical Activation of H_2: Photoreduction of $Rh^I(CO)_2/Al_2O_3$ by H_2

Edward A. Wovchko and John T. Yates, Jr.*

Contribution from the Surface Science Center, Department of Chemistry, University of Pittsburgh, Pittsburgh, Pennsylvania 15260

Received August 18, 1995[⊗]

Abstract: The UV (325 nm) photolysis of atomically-dispersed $Rh^I(CO)_2$ species supported on an Al_2O_3 surface in the presence of H_2 causes a reduction process producing Rh^0_x surface species at 200 K. The Rh^0_x sites are detected by means of the adsorption of characteristic chemisorbed CO species. The H−H bond is activated by the unstable and coordinatively unsaturated Rh^ICO surface intermediate generated during photodecomposition of $Rh^I(CO)_2$. The results indicate that mobile Rh-containing surface species are produced photolytically from isolated $Rh^I(CO)_2$ and proceed to form Rh^0_x clusters; this phenomenon offers a new method for the control of metal dispersion on supported catalysts.

1. Introduction

The photochemically-generated $Rh^I(CO)$ surface species exhibits a coordinatively-unsaturated 16-electron center which can activate the C−H bonds in alkanes.[1−4] Similar centers have been photochemically produced in homogeneous phase, and these centers are also able to activate C−H bonds in alkanes.[5−9] In this paper we demonstrate that the same surface species produced by the photochemical destruction of atomically-dispersed $Rh^I(CO)_2$ supported on an Al_2O_3 surface is able to activate the H−H bond of molecular hydrogen. It is postulated that surface carbonyl hydride intermediates of the formula $Rh(CO)H_x$ ($x = 1, 2$) are produced. The formation of the carbonyl hydride species is a critical first step in the photoreduction of the Rh^I-based surface species to produce metallic Rh cluster sites, designated Rh^0_x.

The parent species for this work is $Rh^I(CO)_2$ on Al_2O_3, designated the rhodium *gem*-dicarbonyl. This species is produced from metallic Rh^0_x during CO adsorption; oxidation to $Rh^I(CO)_2$ occurs by means of the involvement of isolated surface Al−OH groups which act as an oxidizing agent.[10−14] The $Rh^I(CO)_2/Al_2O_3$ sites are the surface analog to homogeneous-phase metal carbonyl species such as $(\eta^5\text{-}C_5Me_5)Rh^I(CO)$.[5−9] $Rh^I(CO)_2$ exhibits two strong carbonyl stretching modes at ~2100 and ~2030 cm^{-1} due to symmetric and antisymmetric coupling.[15−23] It has been demonstrated previously that photochemical activation of $Rh^I(CO)_2/Al_2O_3$ produces $Rh^I(CO)/Al_2O_3$ which can activate C−H bonds in both cyclohexane[1−3] and methane[4], forming an unstable Rh(CO)(H)(R) species, where R = $-C_6H_{11}$ or $-CH_3$. In addition, a competitive side reaction of $Rh^I(CO)$ occurs when this chemically active species reacts with undecomposed $Rh^I(CO)_2$ to produce $Rh_2(CO)_3/Al_2O_3$.[3]

Activation of the H−H bond in H_2 is of central importance in many sorts of catalytic hydrogenation reactions. On transition metal surfaces, H−H bond activation occurs spontaneously, and the dissociated species are active in the hydrogenation of many sorts of atoms and molecules,[24] such as CO,[25−28] CO_2,[29−31] unsaturated hydrocarbons,[24] adsorbed nitrogen,[32] and sulfur.[33] These exposed metal surface sites are coordinatively unsaturated sites, akin in a way to coordinatively-unsaturated $Rh^I(CO)/Al_2O_3$ sites made photochemically.

Several infrared studies of H_2 adsorption on supported metallic Rh catalysts have been reported.[34−36] Hydrogen

[⊗] Abstract published in *Advance ACS Abstracts,* December 1, 1995.

(1) Ballinger, T. H.; Yates, J. T., Jr. *J. Am. Chem. Soc.* **1992**, *114*, 10074.
(2) Ballinger, T. H.; Yates, J. T., Jr. *J. Phys. Chem.* **1992**, *96*, 9979.
(3) Wong, J. C. S.; Yates, J. T., Jr. *J. Am. Chem. Soc.* **1994**, *116*, 1610.
(4) Wong, J. C. S.; Yates, J. T., Jr. *J. Phys. Chem.* in press.
(5) Rest, A. J.; Whitwell, I.; Graham, W. A. G.; Hoyano, J. K.; McMaster, A. D. *J. Chem. Soc., Chem. Commun.* **1984**, *1984*, 624.
(6) Rest, A. J.; Whitwell, I.; Graham, W. A. G.; Hoyano, J. K.; McMaster, A. D. *J. Chem. Soc., Dalton. Trans.* **1987**, *1987*, 1181.
(7) Weiller, B. H.; Wasserman, E. P.; Bergman, R. G.; Moore, C. B.; Pimentel, G. C. *J. Am. Chem. Soc.* **1989**, *111*, 8288.
(8) Schultz, R. H.; Bengali, A. A.; Tauber, M. J.; Weiller, B. H.; Wasserman, E. P.; Kyle, K. R.; Moore, C. B.; Bergman, R. G. *J. Am. Chem. Soc.* **1994**, *116*, 7369.
(9) Bengali, A. A.; Schultz, R. H.; Moore, C. B.; Bergman, R. G. *J. Am. Chem. Soc.* **1994**, *116*, 9585.
(10) Basu, P.; Panayotov, D.; Yates, J. T., Jr. *J. Phys. Chem.* **1987**, *91*, 3133.
(11) Basu, P.; Panayotov, D.; Yates, J. T., Jr. *J. Am. Chem. Soc.* **1988**, *110*, 2074.
(12) Paul, D. K.; Ballinger, T. H.; Yates, J. T., Jr. *J. Phys. Chem.* **1990**, *94*, 4617.
(13) Ballinger, T. H.; Yates, J. T., Jr. *J. Phys. Chem.* **1991**, *95*, 1694.
(14) Zaki, M. I.; Ballinger, T. H.; Yates, J. T., Jr. *J. Phys. Chem.* **1991**, *95*, 4028.
(15) Yang, A. C.; Garland, C. W. *J. Phys. Chem.* **1957**, *61*, 1504.
(16) Yates, J. T., Jr.; Duncan, T. M.; Worley, S. D.; Vaughan, R. W. *J. Chem. Phys.* **1979**, *70*, 1219.
(17) Yates, J. T., Jr.; Duncan, T. M.; Vaughan, R. W. *J. Chem. Phys.* **1979**, *71*, 3908.
(18) Antoniewicz, P. R.; Cavanagh, R. R.; Yates, J. T., Jr. *J. Chem. Phys.* **1980**, *73*, 3456.
(19) Cavanagh, R. R.; Yates, J. T., Jr. *J. Chem. Phys.* **1981**, *74*, 4150.
(20) Yates, J. T., Jr.; Kolasinski, K. *J. Chem. Phys.* **1983**, *79*, 1026.
(21) Rice, C. A.; Worley, S. D.; Curtis, C. W.; Guin, J. A ; Tarrer, A. R. *J. Chem. Phys.* **1981**, *74*, 6487.
(22) Solymosi, F.; Pásztor, M. *J. Phys. Chem.* **1985**, *89*, 4789.
(23) Solymosi, F.; Knözinger, H. *J. Chem. Soc., Faraday Trans. 2* **1990**, *86*, 389.
(24) *Hydrogen Effects in Catalysis*; Paál, Z., Menon, P. G., Eds.; Marcel Dekker, Inc.: New York and Basel, 1988.
(25) Bonzel, H. P.; Krebs, H. J. *Surf. Sci.* **1982**, *117*, 639.
(26) Solymosi, F.; Pásztor, M. *J. Phys. Chem.* **1986**, *90*, 5312.
(27) Worley, S. D.; Mattson, G. A.; Caudill, R. *J. Phys. Chem.* **1983**, *87*, 1671.
(28) Chuang, S. S. C.; Pien, S. I. *J. Catal.* **1992**, *135*, 618.
(29) Henderson, M. A.; Worley, S. D. *J. Phys. Chem.* **1985**, *89*, 1417.
(30) Solymosi, F.; Pásztor, M. *J. Catal.* **1987**, *104*, 312.
(31) Solymosi, F.; Erdöhelyi, A.; Kocsis, M. *J. Catal.* **1980**, *65*, 428.
(32) Ertl, G. In *Catalysis, Science and Technology*; Anderson, J. R., Boudart, M., Eds.; Springer-Verlag: Berlin, 1983; Vol. 4, Chapter 3, pp 257−276.
(33) Vrinat, M. L. *Appl. Catal.* **1983**, *6*, 137.
(34) Pei, Z.; Fang, T. H.; Worley, S. D. *J. Phys. Chem.* **1995**, *99*, 3663.

0002-7863/95/1517-12557$09.00/0

adsorbs on Rh/Al_2O_3 (298−373 K) at high pressures (1000−8000 Torr) and gives a very weak infrared band at 2013 cm^{-1} for the Rh−H stretching mode.[34,35] Hydrogenation studies of CO and CO_2 over Rh/Al_2O_3 provide evidence for a stable Rh(CO)(H) species with a Rh−CO stretching mode at 2036 cm^{-1}.[23,26,27,29−31] This species was generated at elevated temperatures (500 K) and was more pronounced at high Rh loadings (up to 10%) where metallic sites dominate.

We have examined the ultraviolet photolysis of $Rh^I(CO)_2/Al_2O_3$ in the presence of a high pressure of H_2 (181 Torr) using similar techniques as those used in previous cyclohexane[1−3] and methane[4] activation studies. Infrared spectroscopy was employed to monitor developments in the carbonyl stretching region. Activation of the H−H bond occurs with subsequent reduction of the rhodium carbonyls, generating reduced rhodium sites (Rh^0_x) at low temperature (200 K). Thus highly dispersed $Rh^I(CO)_2$ can be photochemically reduced to metallic Rh sites using the methods described here.

2. Experimental Section

The transmission infrared cell used for the photoreduction of $Rh^I(CO)_2/Al_2O_3$ was described in detail previously.[37,38] The cell is constructed from a stainless steel cube with six conflat flange ports. Two ports have double viton O-ring-sealed, differentially pumped, KBr windows. Samples spray deposited onto a tungsten support grid (0.0254 mm thick containing 0.022 mm square openings) were mounted in the center of the cell on electrical feedthrough leads. The cell could be translated laterally for proper background and sample scans. Sample cooling was achieved by filling a reentrant Dewar with liquid nitrogen. A digital temperature programmer/controller was used for electrical heating for maintaining constant temperatures in the range 150 to 1500 ± 2 K.[39] Temperatures were measured by a K-type thermocouple spot welded on the top center of the tungsten grid. The cell was connected to a bakeable stainless steel vacuum system pumped by 60 L s^{-1} turbomolecular and 30 L s^{-1} ion pumps (base pressure $<1 \times 10^{-8}$ Torr). Gas pressures were measured with a MKS 116A Baratron capacitance manometer (range 10^{-3} to 10^3 Torr). A Dycor M100M quadrupole mass spectrometer was used for gas analysis and leak checking.

The 0.5% Rh/Al_2O_3 samples were prepared by dissolving $RhCl_3 \cdot 3H_2O$ (Alfa 99.9% pure) in ultrapure H_2O (10 mL/g of support). The solution was then mixed with the appropriate amount of powdered Al_2O_3 (Degussa, 101 m^2/g) and ultrasonically dispersed for approximately 45 min. The slurry was mixed with acetone (Mallinckrodt, AR) (9/1 acetone/H_2O volume ratio) and sprayed onto the warmed (~330 K) tungsten grid using a nitrogen-gas-pressurized atomizer. This mixture was sprayed on two-thirds (3.6 cm^2) of the grid leaving a shielded one-third section (1.8 cm^2) open for background scans. Spraying was interrupted intermittently to allow for solvent evaporation. The amount of sample deposited could be regulated by adjusting the total spraying time to give deposits ranging from 24 to 35 mg (6.7 to 9.7 mg/cm^2).

After spraying, the grid containing the sample was transferred into the infrared cell and evacuated at 475 K for 15 to 21 h prior to reduction. Reduction of the sample was carried out at 475 K using four exposures (15, 30, 45, 60 min) of 190 Torr of H_2 (Matheson 99.9995% pure) followed by evacuation after each exposure. The reduced sample was outgassed at 475 K for at least another 18 h. The sample was then cooled to 303 K and exposed to 10 Torr of CO for 10 min to convert the reduced rhodium to $Rh^I(CO)_2$. After exposure, the cell was evacuated and cooled to 200 K for photolysis experiments. The temperature was maintained at 200 ± 2 K for the duration of each high gas pressure experiment. The temperature did not exceed 202 K for the vacuum experiment.

All infrared spectra were recorded using a nitrogen-gas-purged Mattson Research Series I Fourier transform infrared spectrometer. The spectrometer was equipped with a liquid nitrogen cooled HgCdTe wide band detector. All spectra were measured by averaging 1000 scans at a spectral resolution of 4 cm^{-1} and a signal gain of 4. Background spectra due to small deposits on the KBr windows were recorded by translating the cell so that the beam passed through the unsprayed section of the grid. Absorbance spectra were obtained by ratioing single beam spectra of the sample to the background single beam spectra. All sample spectra were recorded at 200 K and 181 Torr of gas pressures (or at pressures $<5 \times 10^{-8}$ Torr for the vacuum experiment).

The ultraviolet light was provided by a 350-W high-pressure mercury arc lamp. The lamp housing is equipped with a F/1 two-element UV fused silica condensing lens, an iris diaphragm, and a shutter. In addition to a 10 cm water infrared radiation filter, a 325 ± 50 nm bandpass filter was utilized. The photoflux of the filtered UV light was 7.4×10^{16} photons cm^{-2} s^{-1} ± 10% as measured by a thermopile. The photochemistry and infrared measurements can be conducted simultaneously without disturbing the position of the cell or UV lamp. The UV source axis is aligned perpendicular to the infrared beam. The UV light passes through a 2.40 cm diameter UV grade sapphire window onto the Rh/Al_2O_3 sample. The grid is aligned at an angle such that both the spectrometer infrared beam and the UV light are focused at a 45° angle to the normal of the grid.

The white-light control experiment was performed with a similar arrangement as the UV-light experiments. In this case the UV lamp was replaced with a tungsten−halogen incandescent lamp (Sylvania XN21, 24 V, 250 W). The water filter was emptied and the 325-nm filter was replaced by a >450 nm bandpass filter. The lamp power was adjusted to achieve a temperature increase slightly greater than the observed temperature increase from UV-light irradiation (1−2 K in the presence of 181 Torr of gas). During these photolysis experiments, electrical feedback temperature control on a small grid heating current was utilized to dampen this temperature increase over a ~30 min period and to re-establish a constant sample temperature of 199.5 K.

Carbon monoxide (Matheson 99.9%) was obtained in a breakseal Pyrex storage bulb and used without further purification. Helium (Matheson 99.9999%) and hydrogen (Matheson 99.9995%) were obtained in cylinders and also used without further purification.

3. Results

1. Photolysis of $Rh^I(CO)_2/Al_2O_3$ in Hydrogen. The UV photolysis of $Rh^I(CO)_2/Al_2O_3$ at 200 K in the presence of 181 Torr of hydrogen gas is presented in Figure 1A. The spectrum measured at $t_{uv} = 0$ min shows the formation of $Rh^I(CO)_2$ species generated upon exposure to CO. A doublet characteristic of this *gem*-dicarbonyl species can be seen at 2099 and 2028 cm^{-1}. These bands are assigned respectively to the symmetric and antisymmetric CO stretching modes of $Rh^I(CO)_2$.[15−23] There is a small broad band at 1827 cm^{-1} assigned to bridge-bound CO on metallic Rh^0_x sites not dispersed to form $Rh^I(CO)_2$ during CO adsorption.[15−23] At the low 0.5% Rh/Al_2O_3 loading studied here, a low-intensity C−O mode at 2061 cm^{-1} is detected, indicating that the coverage of terminally-bound Rh−CO species on metallic Rh^0_x sites is small. The predominant IR absorbance is due to $Rh^I(CO)_2$.

After generating $Rh^I(CO)_2$ species, the sample was irradiated with UV light in the presence of H_2(g). Transformations in the carbonyl stretching region can be seen in the spectra measured at 15, 60, and 360 min during the photolysis. Depletion of the 2099- and 2028-cm^{-1} bands was accompanied by the development of bands at 2061, 1977, and 1827 cm^{-1}. Three isosbestic absorbance crossing points are observed at 2083, 2037, and 2000 cm^{-1}. These transformations are caused by the conversion of $Rh^I(CO)_2$ to both terminally, and bridge-

(35) Wey, J. P.; Neely, W. C.; Worley, S. D. *J. Phys. Chem.* **1991**, *95*, 8881.
(36) McKee, M. L.; Dai, C. H.; Worley, S. D. *J. Phys. Chem.* **1988**, *92*, 1056.
(37) Basu, P.; Ballinger, T. H.; Yates, J. T., Jr. *Rev. Sci. Instrum.* **1988**, *59*, 1321.
(38) Wong, J. C. S.; Linsebigler, A.; Lu, G.; Fan, J.; Yates, J. T., Jr. *J. Phys. Chem.* **1995**, *99*, 335.
(39) Muha, R. J.; Gates, S. M.; Yates, J. T., Jr.; Basu, P. *Rev. Sci. Instrum.* **1985**, *56*, 613.

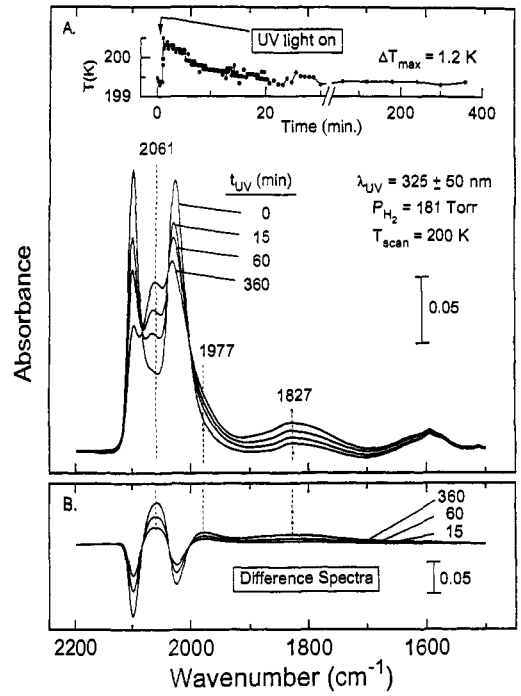

Figure 1. (A) Infrared spectra measured in the C−O stretching region during the photoreduction of $Rh^I(CO)_2/Al_2O_3$ in the presence of 181 Torr of H_2 at 200 K. (B) Difference spectra, subtracting the spectrum measured at $t_{uv} = 0$ min. The temperature recorded during photolysis is shown in the inset of (A). (Spectra have been baseline corrected.)

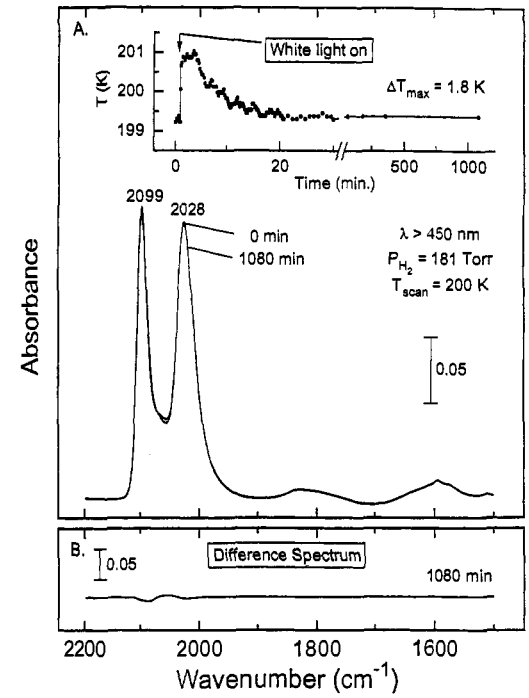

Figure 2. (A) Infrared spectra of the C−O region recorded before and after 1080 min of white light irradiation of $Rh^I(CO)_2/Al_2O_3$ in 181 Torr of H_2 at 200 K. (B) Difference spectrum after 1080 min of white light irradiation. The temperature recorded during photolysis is shown in the inset of (A). Note that the absorbance scales are identical for Figures 1A and 2A and Figures 1B and 2B. (Spectra have been baseline corrected.)

bound carbonyl species on metallic Rh^0_x sites. The spectrum measured after 360 min of photolysis remains essentially unchanged after UV irradiation is stopped and the cell is evacuated at 200 K. This indicates that at 200 K the resulting rhodium carbonyl species are stable on the surface.

The difference spectra for the experiment displayed in Figure 1A are shown in Figure 1B. Here, the spectrum measured at $t_{uv} = 0$ min has been subtracted from the spectra achieved following UV irradiation. The formation of the 2061-cm^{-1} feature and loss of the $Rh^I(CO)_2$ doublet is clearly seen. One can observe the growth of the 1977- and 1827-cm^{-1} bands as well. Exposure of the sample to UV light caused an immediate increase in temperature of approximately 1.2 K in the presence of H_2 gas as shown in the upper inset of Figure 1A. During the photolysis, the electrical feedback controller gradually adjusted the small electrical heating current output until the original set point temperature near 199.5 K was reached (total re-establishment time was about 30 min).

2. Control Experiment: White Light Irradiation. To prove that the transformation observed in Figure 1 was a UV photoeffect and not a thermal effect, an incandescent lamp providing filtered white light (above $\lambda = 450$ nm) was employed in a control experiment. The white light irradiation of $Rh^I(CO)_2/Al_2O_3$ in the presence of H_2 (g) at 181 Torr of pressure is presented in Figure 2. An initial 1.8 K sample temperature increase was observed in the temperature profile of Figure 2A and the temperature controller then gradually reestablished the set point temperature of 199.5 K. The spectra measured before white light irradiation and after 1080 min show virtually no change in the 2099- and 2028-cm^{-1} bands. These results demonstrate conclusively that the effect seen in Figure 1 is indeed an ultraviolet photoeffect and is not a thermal effect.

3. Control Experiments: UV Photolysis under Helium and in Vacuum. A factor critical to the explanation of the transformations observed in Figure 1 is the role of the H_2 (D_2). Two control experiments were done to verify that hydrogen is a crucial reactant in the conversion of $Rh^I(CO)_2$ to other Rh−CO species. These are (1) the photolysis of $Rh^I(CO)_2/Al_2O_3$ in the presence of 181 Torr He and (2) photolysis under vacuum. Helium was chosen to provide a similar flux of gas molecules to the sample without the chemical influence of H_2. The difference spectra measured after 360 min of UV photolysis for (a) H_2, (b) He, and (c) under vacuum are shown in Figure 3. Scaling factors, in the range 1.12−0.83, based on the initial ($t_{uv} = 0$ min) absorbance of the 2099-cm^{-1} symmetric $Rh^I(CO)_2$ mode, have been applied to spectra (b) and (c), respectively. The scaling factors result in the normalization of the 2099-cm^{-1} band to the initial absorbance value at $t_{uv} = 0$ min for the photolysis experiment in H_2. One can see that the loss of $Rh^I(CO)_2$ was less prevalent in the He and vacuum experiments compared to the H_2 experiment. There is also much less development of the 2061-cm^{-1} feature under He or in vacuum, and for the He or vacuum conditions there was essentially no development of the 1827-cm^{-1} feature. The band at 1977 cm^{-1} is, however, present in each case at comparable intensities indicating that H_2 is not responsible for the 1977-cm^{-1} band observed in spectrum (a).

4. Hydrogen and Deuterium Photoactivation. The possibility of Rh−H bond formation during photolysis was investigated as shown in Figure 4. Rhodium hydride infrared absorbance bands at approximately 2013 cm^{-1} for Rh−H[34-36] and the RhC−O mode at 2036 cm^{-1} have been reported for Rh(CO)(H).[23,26,27,29-31] These features severely overlap with the strong Rh−C−O modes.[15-23,26,27,29-31] In an attempt to identify possible Rh−H features absorbing in the 2100−2000-cm^{-1} region, the photochemistry of $Rh^I(CO)_2$ under deuterium was studied. Figure 4 shows the 360 min difference spectra of identical H_2 and D_2 photoactivation experiments performed on two separate samples with similar Rh/Al_2O_3 optical densities (1% less for D_2 experiment). Both difference spectra display essentially the same bands of nearly equivalent intensities

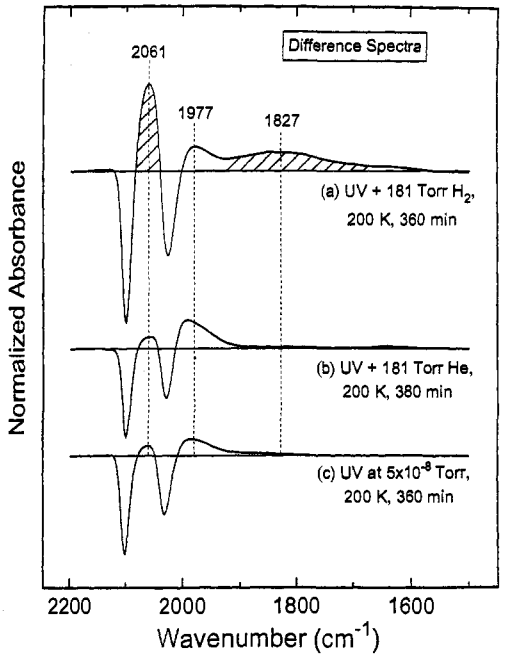

Figure 3. Control experiments for H_2 photoreduction. (a) The difference spectrum (from Figure 1B) measured after 360 min of UV photoactivation in H_2. (b) The normalized difference spectrum measured after 360 min of UV photolysis in the presence of 181 Torr of He at 200 K. (c) The normalized difference spectrum measured after 360 min of photodecomposition of $Rh^I(CO)_2/Al_2O_3$ while pumping at 5×10^{-8} Torr. (Spectra have been baseline corrected.)

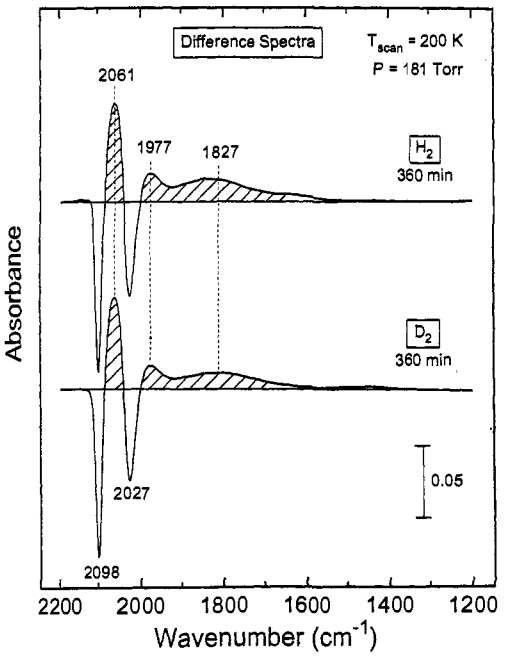

Figure 4. Infrared difference spectra measured after 360 min of UV photolysis in H_2 (from Figure 1B) and in D_2 over $Rh^I(CO)_2/Al_2O_3$. (Spectra have been baseline corrected.)

indicating that Rh−H modes are not visible when photolysis under H_2 occurs. No significant features, typical for Rh−D species, around 1440 cm^{-1} were detected here when D_2 gas was used. The negative 2099- and 2028-cm^{-1} doublet and the positive 2061-, and 1827-cm^{-1} bands (indicated by cross-hatching) clearly show the conversion of the *gem*-dicarbonyl to terminally- and bridge-bound rhodium carbonyl species. In both cases a positive feature was also observed at 1977 cm^{-1}.

4. Discussion

1. Photochemistry of $Rh^I(CO)_2/Al_2O_3$. Large changes occur in the infrared spectrum of $Rh^I(CO)_2/Al_2O_3$ during UV photolysis in the presence of H_2 (Figure 1). It is clear from previous mass spectrometric and infrared spectroscopic studies[1,2] that CO is photodesorbed from a surface consisting primarily of $Rh^I(CO)_2$ species. The results of Figure 2 demonstrate that the photoreduction in H_2 is clearly caused by ultraviolet photons ($\lambda \approx 325 \pm 50$ nm) and not by visible photons ($\lambda > 450$ nm) delivering a similar amount of thermal energy to the surface.

The most logical primary species which can be produced by UV irradiation of $Rh^I(CO)_2$ is $Rh^I(CO)$, possessing a 16-electron, coordinatively-unsaturated center. This center is highly reactive both in homogeneous phase and on surfaces, causing C−H bond scission in alkanes.[1-9] We propose that the H−H bond in H_2 can be similarly activated by $Rh^I(CO)$, producing $Rh(CO)H_x$ ($x \approx 1,2$). This intermediate species, not observed in our IR measurements, is mobile and is a precursor to metallic Rh^0_x formation.

Infrared spectroscopy studies of CO chemisorption on Rh/Al_2O_3 containing higher concentrations of Rh (yielding metallic Rh^0_x sites) than in the experiments reported here reveal the existence of two basic types of chemisorbed CO: (1) terminal CO on Rh^0_x, and (2) bridged CO on Rh^0_x. The range of carbonyl frequencies for terminal CO on Rh^0_x sites is 2042−2076 cm^{-1} depending on the Rh loadings and the CO coverage.[16,17,19-22] The range of carbonyl frequencies for bridging CO on Rh^0_x sites is 1825−1900 cm^{-1}.[16,17,19-22] On the basis of many studies of CO chemisorption on metallic Rh sites, we assign the 2061-cm^{-1} CO frequency to terminally bound CO on Rh^0_x sites. We assign the 1827-cm^{-1} CO frequency to bridge-bonded CO on Rh^0_x sites.

The production of the 1977-cm^{-1} carbonyl stretching mode is observed in all $Rh^I(CO)_2$ photoactivation experiments carried out under H_2, D_2, and He and in vacuum. As shown in Figure 3, its production does not correlate with the production of either terminal CO or bridged CO on metallic Rh^0_x sites, indicating that the 1977-cm^{-1} mode is unrelated to the H_2-induced photoreduction of $Rh^I(CO)_2$ species to Rh^0_x. Furthermore, the 1977-cm^{-1} mode is not a Rh−H mode since its development is identical when photolysis occurs under either H_2 or D_2. We therefore postulate that the 1977-cm^{-1} mode is associated with the reaction of the photoproduced mobile $Rh^I(CO)$ with unphotolyzed $Rh^I(CO)_2$ to produce a non-metallic $Rh_2(CO)_3$ dimer species. The 1977-cm^{-1} mode is assigned to a terminal CO ligand in $Rh_2(CO)_3$ while the bridging CO in $Rh_2(CO)_3$ may be hidden in the broad band centered at 1827 cm^{-1}. Wong and Yates[3] saw a similar band develop at 1987 cm^{-1} during $Rh^I(CO)_2$ photolysis under cyclohexane which was also assigned to $Rh_2(CO)_3$.

An alternate model, in which H spillover from H_2 dissociation on Rh^0_x sites causes neighboring Rh^I reduction, was tested using much more highly dispersed $Rh^I(CO)_2$ preparations from 0.05% Rh/Al_2O_3 (experiments not shown). The effects seen here are also found under the high-dispersion conditions where metallic Rh^0_x sites are not present at the beginning of the photochemical experiment.

2. Lack of Observation of Rh−H Stretching Modes. The experiments of Figure 4 involving the photolysis of $Rh^I(CO)_2/Al_2O_3$ under H_2 and D_2 are conclusive in showing that spectral developments in the 1700−2100-cm^{-1} region do not involve Rh−H vibrational modes. No significant variation in the difference spectral developments occurs when D_2 is substituted for H_2 in these experiments. This observation suggests that $Rh^I(CO)H_x$ ($x = 1,2$) species are transient in nature at 200 K and

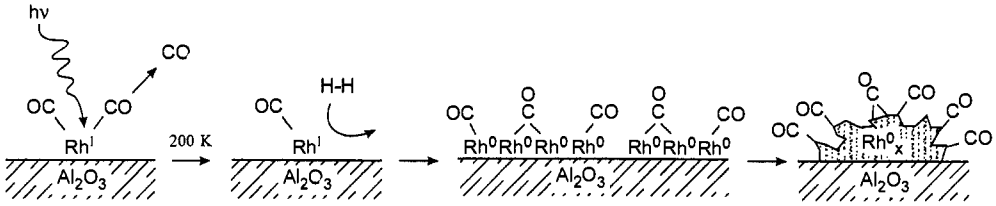

Figure 5. Proposed reaction scheme for the photoreduction of $Rh^I(CO)_2/Al_2O_3$ at 200 K by H_2.

cannot be observed by infrared spectroscopy in either the CO stretching region or the Rh−H stretching region. This conclusion is confirmed by our photoactivation studies with D_2, where modes in the 1200−1500-cm^{-1} range due to Rh−D species are also not observed (Figure 4).

These observations differ from work done on metallic Rh^0_x surfaces, where weak Rh−H vibrational modes have been observed following H_2 dissociative chemisorption. For example, Worley and co-workers[34,35] have measured by infrared spectroscopy the presence of a Rh−H stretching mode at 2013 cm^{-1} in high-pressure H_2 studies on Rh^0_x/Al_2O_3 surfaces. The intensity of this mode was weak relative to the infrared bands reported in this work. In earlier studies, Worley and co-workers[27,29] reported a strong band a 2036 cm^{-1} during CO and CO_2 hydrogenation over Rh^0_x/Al_2O_3 surfaces at elevated temperatures (500 K). They attributed this band to a rhodium carbonyl hydride, Rh(CO)H. Solymosi and co-workers also reported similar results.[23,26,30,31]

3. H−H Bond Activation on a Coordinatively Unsaturated Site. It is well established that $Rh^I(CO)_2$ exists as an isolated, atomically-dispersed species on Al_2O_3 surfaces.[13−23,40−43] By analogy to homogeneous phase photochemistry of metal carbonyls,[5−9] photolysis of isolated $Rh^I(CO)_2/Al_2O_3$ will produce $Rh^I(CO)/Al_2O_3$ also. We have previously shown that C−H bond activation occurs on $Rh^I(CO)/Al_2O_3$ centers in an analogous fashion to the homogenous phase behavior of photochemically-produced coordinatively-unsaturated species like (η^5-C_5Me_5)$Rh^I(CO)$. We therefore propose that the isolated $Rh^I(CO)/Al_2O_3$ site is capable of H−H bond activation also. The formation of a three-center bond

is postulated, leading to the rupture of the H−H bond by analogy to similar processes involving C−H bonds. Such H−H activation processes are also found in homogeneous phase organometallic chemistry.[44−47]

4. Photoreduction of $Rh^I(CO)/Al_2O_3$ to Rh^0_x/Al_2O_3. Based on our observation of the formation of metallic Rh^0_x/Al_2O_3 sites by the photoreduction of $Rh^I(CO)_2$ in H_2, we propose that mobile Rh-containing species are produced following photochemical activation. These species coalesce into Rh^0_x/Al_2O_3 even at 200 K. Thus, the photochemical ejection of a CO ligand in the presence of H_2(g) leads to Rh^0_x cluster formation; these Rh^0_x clusters are detected through the formation of characteristic chemisorbed CO species. A schematic diagram of the surface process which occurs is shown in Figure 5. This behavior is analogous to the formation of polynuclear metal carbonyls in the homogeneous phase following photochemical release of a CO ligand.[48] The photochemical reaction and agglomeration of $Rh^I(CO)_2$-based surfaces may provide a new way for the control of catalyst preparation in which highly dispersed catalysts may be photoreduced to metallic catalysts of lower dispersion.

5. Conclusions

The photoreduction of $Rh^I(CO)_2/Al_2O_3$ by H_2 has been studied using transmission infrared spectroscopy. The following conclusions can be made:

(1) Infrared bands at 2061 and 1827 cm^{-1} attributed to terminally- and bridge-bound CO species on metallic Rh sites were observed to intensify during the ultraviolet photolysis of atomically-dispersed $Rh^I(CO)_2/Al_2O_3$ in H_2 at 200 K.

(2) The reaction occurs when H_2 is activated on the photochemically-produced coordinatively-unsaturated Rh^I center ultimately causing the reduction of $Rh^I(CO)_2$ to Rh^0_x according to the reaction scheme shown in Figure 5.

(3) A carbonyl stretching mode at 1977 cm^{-1} was detected during the photolysis under H_2, He, and vacuum and is assigned to a side reaction involving photochemically-produced $Rh^I(CO)$ and $Rh^I(CO)_2$ to produce $Rh_2(CO)_3$ species.

(4) This method provides a new method for control of catalyst dispersion not involving thermal activation.

Acknowledgment. We thank Gidget Cantrell for performing some initial experiments. Financial support from the Department of Energy, Office of Basic Energy Sciences is acknowledged with thanks.

JA952851Q

(40) Robbins, J. L. *J. Phys. Chem.* **1986**, *90*, 3381.
(41) Thayer, A. M.; Duncan, T. M. *J. Phys. Chem.* **1989**, *93*, 6763.
(42) van't Blik, H. F. J.; van Zon, J. B. A. D.; Huizinga, T.; Vis, J. C.; Koningsberger, D. C.; Prins, R. *J. Am. Chem. Sac.* **1985**, *107*, 3139.
(43) van't Blik, H. F. J.; van Zon, J. B. A. D.; Huizinga, T.; Vis, J. C.; Koningsberger, D. C.; Prins, R. *J. Phys. Chem.* **1983**, *87*, 2264.
(44) Dickson, R. S. *Homogeneous Catalysis with Compounds of Rhodium and Iridium*; D. Reidel Publishing Co.: Dordrecht, Holland, 1985.
(45) Duckett, S. B.; Newell, C. L.; Eisenberg, R. *J. Am. Chem. Soc.* **1994**, *116*, 10548.
(46) Kunin, A. J.; Johnson, C. E.; Maguire, J. A.; Jones, W. D.; Eisenberg, R. *J. Am. Chem. Soc.* **1987**, *109*, 2963.
(47) Zhou, P.; Vitale, A. A.; Filippo, J. S., Jr.; Saunders, W. H., Jr. *J. Am. Chem. Soc.* **1985**, *107*, 8049.
(48) Cotton, F. A.; Wilkinson, G. *Advanced Inorganic Chemistry*; John Wiley & Sons, Inc.: New York, 1988; Chapter 22.